

Testing the three-dimensional IRI-SIRMUP-P mapping of the ionosphere for disturbed periods

M. Pezzopane^{a,*}, M. Pietrella^a, A. Pignatelli^a, B. Zolesi^a, Lj.R. Cander^b

^a *Istituto Nazionale di Geofisica e Vulcanologia, Via di Vigna Murata 605, 00143 Rome, Italy*

^b *STFC, Rutherford Appleton Laboratory, Chilton, OX11 0QX, UK*

Available online 5 December 2012

Abstract

This paper describes the three-dimensional (3-D) electron density mapping of the ionosphere given as output by the assimilative IRI-SIRMUP-P (ISP) model for three different geomagnetic storms. Results of the 3-D model are shown by comparing the electron density profiles given by the model with the ones measured at two testing ionospheric stations: Roquetes (40.8°N, 0.5°E), Spain, and San Vito (40.6°N, 17.8°E), Italy. The reference ionospheric stations from which the autoscaled f_oF_2 and $M(3000)F_2$ data as well as the real-time vertical electron density profiles are assimilated by the ISP model are those of El Arenosillo (37.1°N, 353.3°E), Spain, Rome (41.8°N, 12.5°E), and Gibilmanna (37.9°N, 14.0°E), Italy. Overall, the representation of the ionosphere made by the ISP model is better than the climatological representation made by only the IRI-URSI and the IRI-CCIR models. However, there are few cases for which the assimilation of the autoscaled data from the reference stations causes either a strong underestimation or a strong overestimation of the real conditions of the ionosphere, which is in these cases better represented by only the IRI-URSI model. This ISP misrepresentation is mainly due to the fact that the reference ionospheric stations covering the region mapped by the model turn out to be few, especially for disturbed periods when the ionosphere is very variable both in time and in space and hence a larger number of stations would be required. The inclusion of new additional reference ionospheric stations could surely smooth out this concern.

© 2012 COSPAR. Published by Elsevier Ltd. All rights reserved.

Keywords: Disturbed ionosphere; Electron density; Ionogram; IRI; Modeling

1. Introduction

The development of models that can provide a comprehensive three-dimensional (3-D) specification of the ionosphere has become more and more important for educational, research, engineering, and civil purposes. For this reason, in the last decade much effort has been devoted to continuously test models that after assimilating observations calculate an updated 3-D image of the ionosphere (Angling and Khattatov, 2006; Thompson et al., 2006; Decker and McNamara, 2007; McNamara et al., 2007, 2008, 2010, 2011; Shim et al., 2011). Moreover, regio-

nal and local models represent an important complement in order to characterize those ionospheric features that may be easily neglected in global models, like the International Reference Ionosphere (IRI) (Bilitza and Reinisch, 2008) and the NeQuick (Radicella, 2009) models. With regard to this, the European Cooperation in Scientific and Technology (COST) actions (Bradley, 1999; Hanbaba, 1999) have demonstrated that regional mapping of the critical frequency of the F2 layer (f_oF_2) and the propagation factor $M(3000)F_2$ is better than the one given by global models. $M(3000)F_2$ is defined as the ratio of the maximum usable frequency at a distance of 3000 km to f_oF_2 , and it represents the secant of the optimum angle at which to broadcast a signal that is to be received at a distance of 3000 km.

Pezzopane et al. (2011) have recently proposed a 3-D regional mapping of the ionosphere based on a

* Corresponding author. Tel.: +39 06 51860525; fax: +39 06 51860397.

E-mail addresses: michael.pezzopane@ingv.it (M. Pezzopane), marco.pietrella@ingv.it (M. Pietrella), alessandro.pignatelli@ingv.it (A. Pignatelli), bruno.zolesi@ingv.it (B. Zolesi), ljiljana.cander@stfc.ac.uk (Lj.R. Cander).

combination of three elements: (1) autoscaled data coming from some reference ionospheric stations, (2) the f_oF2 and $M(3000)F2$ regional grids calculated by the Simplified Ionospheric Regional Model Updated (SIRMUP) (Zolesi et al., 2004; Tsgouri et al., 2005), and (3) the IRI model. The procedure was named as the IRI-SIRMUP-P (ISP) model. In their work, the authors tested the ISP model for geomagnetically quiet conditions, for quasi-stationary ionospheric conditions and at the solar terminator, in a central Mediterranean area extending in latitude from 30° to 44° and in longitude from -5° to 40° , with a $1^\circ \times 1^\circ$ resolution, which is right the validity area of the regional SIRMUP model. The reference ionospheric stations considered by the authors were those of Rome (41.8°N , 12.5°E), and Gibilmanna (37.9°N , 14.0°E), Italy. Pezzopane et al. (2011) showed that mostly at the solar terminator the electron densities calculated by the ISP model were more representative of the real conditions of the ionosphere than those calculated by the IRI model.

In this paper, besides Rome and Gibilmanna, an additional reference ionospheric station was considered, El Arenosillo (37.1°N , 353.3°E), Spain. Moreover, unlike the preliminary study performed by Pezzopane et al. (2011), the test of the model, always in the above mentioned area, was this time done for geomagnetically disturbed conditions. The attention was in fact focused on three different geomagnetic storms occurred in April 2008 (smoothed sunspot number $R_{12} = 3.3$), in April 2010 ($R_{12} = 15.4$), and in May 2010 ($R_{12} = 16.3$), hence for very low solar activity.

In the previous study, the model calculations were validated by comparing the corresponding vertical electron density profiles with those directly measured at some testing ionospheric stations. In this study, due to their relative proximity to at least one of the reference stations, we decided to consider as testing sites the two ionospheric

stations of Roquetes (40.8°N , 0.5°E), Spain, and San Vito (40.6°N , 17.8°E), Italy (Fig. 1).

2. Brief recall of the ISP model

The initial step of the ISP model consists of checking the autoscaling performed at the reference ionospheric stations. In our study, the autoscaling performed by Autoscala (Pezzopane and Scotto, 2005, 2007; Scotto, 2009; Scotto et al., 2012) on the ionograms recorded by the AIS-INGV (Advanced Ionospheric Sounder-Istituto Nazionale di Geofisica e Vulcanologia) ionosonde (Zuccheretti et al., 2003) installed at the ionospheric stations of Rome and Gibilmanna, and the autoscaling performed by the Automatic Real-Time Ionogram Scaler with True height analysis (ARTIST) system (Reinisch and Huang, 1983; Reinisch et al., 2005; Galkin and Reinisch, 2008) on the ionograms recorded by the digisonde (Bibl and Reinisch, 1978) installed at the ionospheric station of El Arenosillo are exploited. If no station has given f_oF2 and $M(3000)F2$ autoscaled values as output, the standard IRI procedure is launched, and a climatological 3-D electron density matrix is generated. Instead, if at least one station has given as output autoscaled values of f_oF2 and $M(3000)F2$, the effective sunspot number (R_{eff}) (Houminer et al., 1993) is calculated on the basis of these values (Zolesi et al., 2004), and it is then used by the Simplified Ionospheric Regional Model (SIRM) (Zolesi et al., 1996) to provide a nowcasting of f_oF2 and $M(3000)F2$ on the regional spatial grid of interest.

In the next step, the f_oF2 and $M(3000)F2$ grids of values computed by the SIRMUP procedure are used as input to IRI, and a 3-D updated matrix of the electron density is generated. At this point, if no reference station has an electron density profile associated with the performed autoscaling, the process stops. Otherwise, if at least one reference

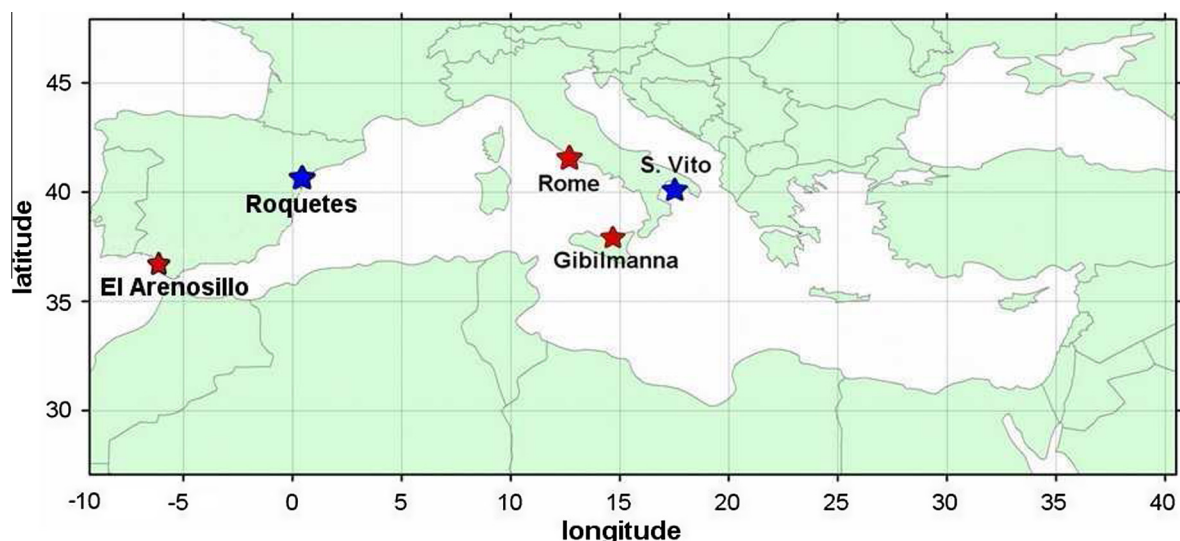


Fig. 1. Map of the central Mediterranean area under study. Red stars represent the ionospheric stations considered as input for the model. Blue stars represent the ionospheric stations considered as test sites.

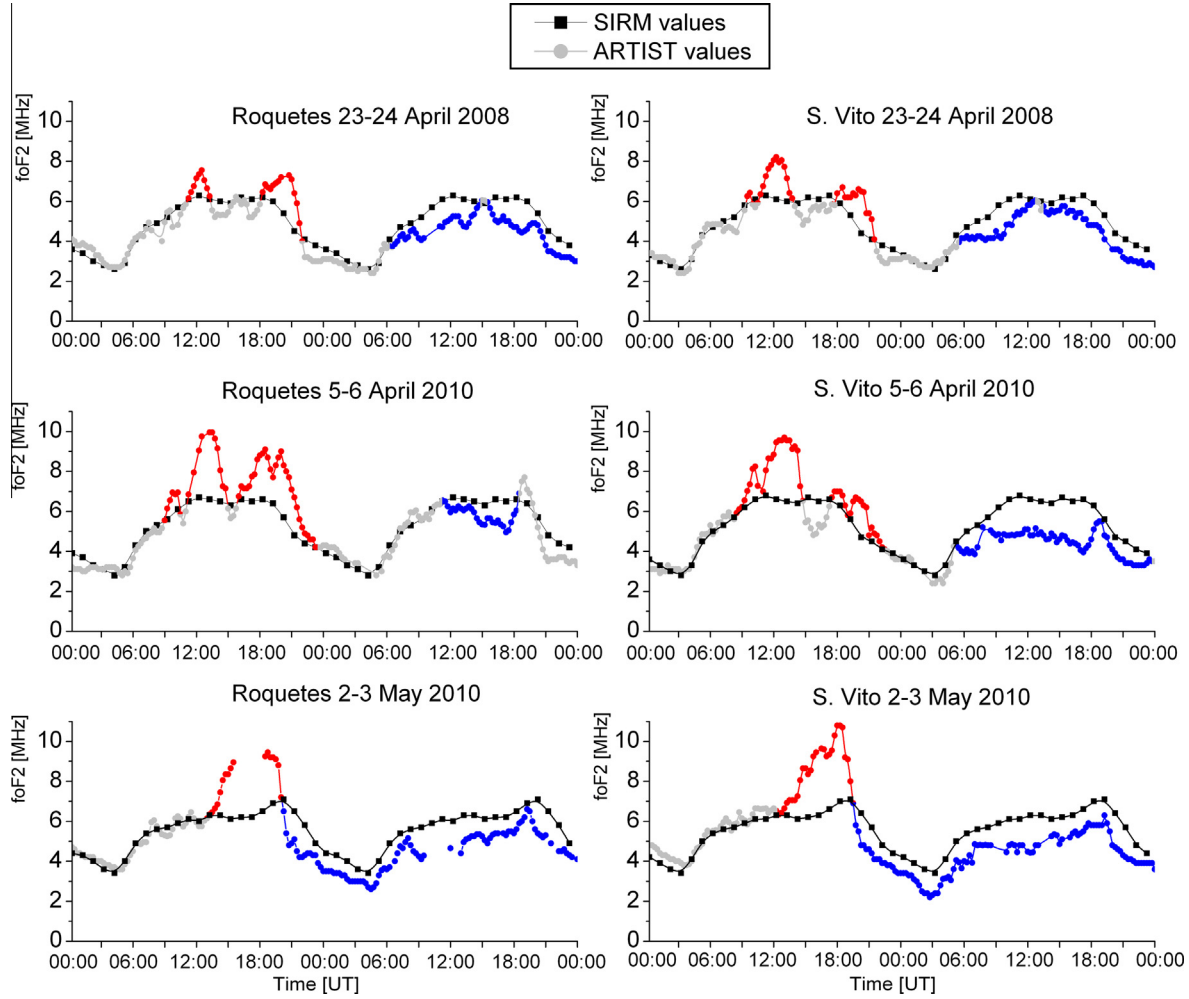


Fig. 2. ARTIST $foF2$ values (grey circles), as obtained by the 15-min ionograms recorded at Roquetes and San Vito from 23 to 24 April 2008, from 5 to 6 April 2010, and from 2 to 3 May 2010, compared to the corresponding $foF2$ hourly median values (black squares) predicted by the SIRM model, both at Roquetes and at San Vito, and here assumed as quiet-day values. The positive and negative ionospheric phases are highlighted by red and blue circles respectively.

ionospheric station has a vertical electron density profile associated with the autoscaling of the ionogram trace, an assimilation process of the measured electron density profiles starts, after which a further updated 3-D electron density matrix is generated. At a definite height, after assimilating the vertical electron density profiles from the reference stations (Pezzopane et al., 2011), the corresponding value T of the electron density at a generic point $x_i(\lambda_i, \theta_i)$ (with $i = 1, \dots, n$, and where λ and θ are the corresponding geographical longitude and latitude) is calculated as follows

$$T[x_i(\lambda_i, \theta_i)] = \sum_{j=1^*}^m \left\{ \exp \left(-\frac{(x_i(\lambda_i, \theta_i) - \bar{x}_j(\lambda_j, \theta_j))^2}{2\sigma^2} \right) M[\bar{x}_j(\lambda_j, \theta_j)] \right. \\ \left. + \left[1 - \exp \left(-\frac{(x_i(\lambda_i, \theta_i) - \bar{x}_j(\lambda_j, \theta_j))^2}{2\sigma^2} \right) \right] I[x_i(\lambda_i, \theta_i)] \right\}; \quad (1)$$

σ is a parameter of the exponential weight function that can be varied, $I[x_i(\lambda_i, \theta_i)]$ is the value of the electron density before assimilating the profiles at the definite height in cor-

respondence of the generic point $x_i(\lambda_i, \theta_i)$. $M[\bar{x}_j(\lambda_j, \theta_j)]$ (with $j = 1^*, \dots, m$, where m represents the number of reference stations) is the measured value of the electron density at the definite height in correspondence of the point $\bar{x}_j(\lambda_j, \theta_j)$ identifying the position of a reference station.

3. Analysis and results

Validation results of the proposed ISP model are here shown by comparing the electron density profiles given by the model with the ones measured at some testing ionospheric stations. As shown in Fig. 1, the reference ionospheric stations considered as input for the model are El Arenosillo, Rome, and Gibilmanna, hence the index m of Eq. (1) is equal to 3^* , while the ionospheric stations considered as test sites are Roquetes and San Vito. The data and the vertical electron density profiles measured at Rome and Gibilmanna are those autoscaled by Autoscala from the ionograms recorded by the AIS-INGV ionosonde, while the data and the electron density profiles measured at El

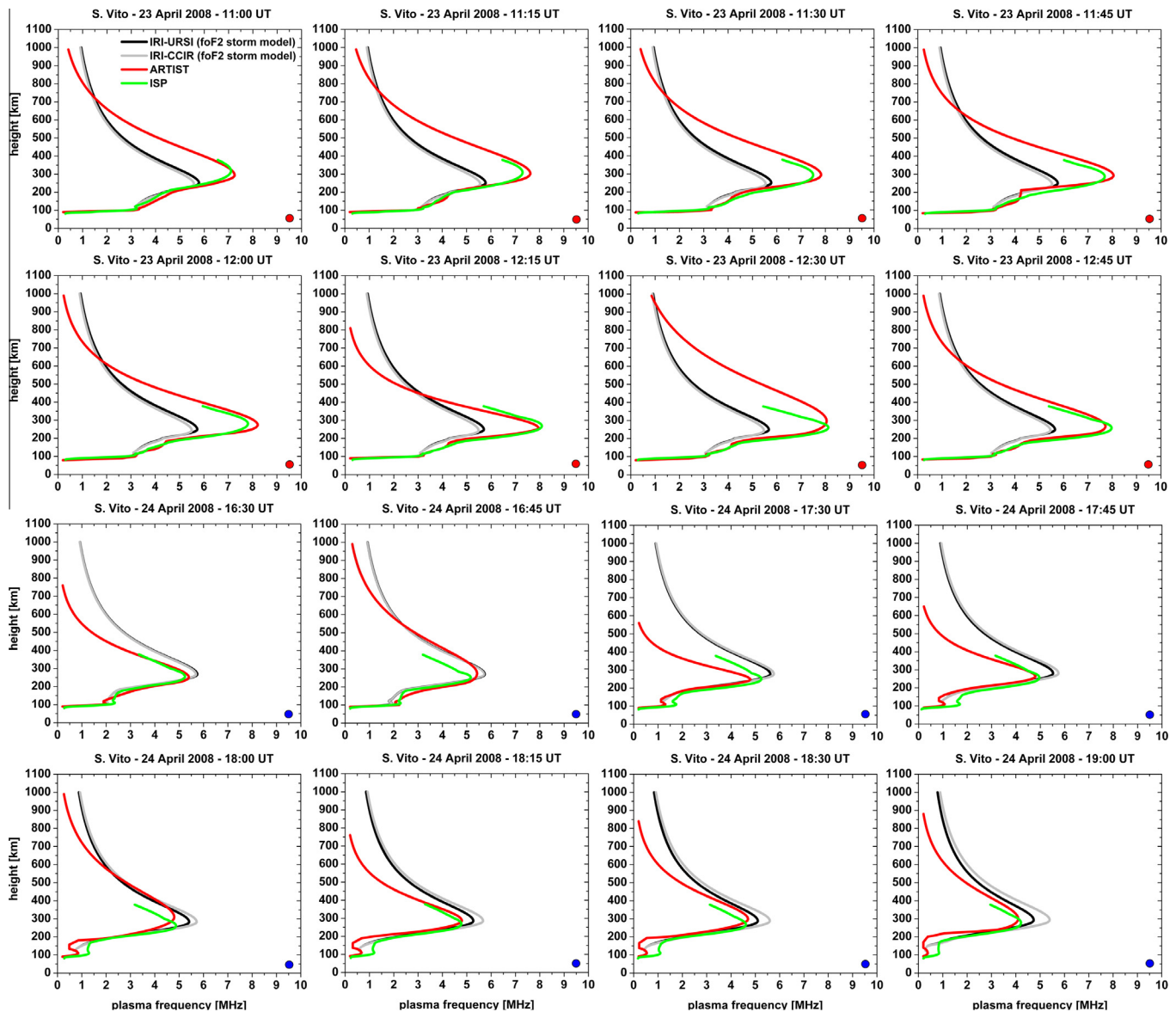


Fig. 3. Comparison among some profiles obtained at S. Vito on 23 and 24 April 2008 by ISP (green), ARTIST (red), IRI-CCIR (gray) and IRI-URSI (black). Red or blue circles close to the lower right angle of the plot identify profiles belonging to the positive or negative ionospheric phase respectively.

Arenosillo, Roquetes, and San Vito, are those autoscaled by ARTIST from the ionograms recorded by the digisonde.

In order to test the model for disturbed ionospheric conditions, the three geomagnetic storms that occurred from 23 to 24 April 2008 (max $K_p = 5$), from 5 to 8 April 2010 (max $K_p = 8$), and from 2 to 4 May 2010 (max $K_p = 6$) were considered. These periods were particularly selected to test the model because most of the autoscaling computations made both by ARTIST at El Arenosillo, Roquetes, and San Vito, and by Autoscala at Rome and Gibilmanna were available. In particular, the attention was focused on the positive and negative ionospheric phases characterizing the disturbed periods under study, as shown in Fig. 2. In this figure to visualize the behavior of the ionosphere during the three geomagnetic storms, the observed 15-min $foF2$ values recorded at Roquetes and San Vito are drawn

in comparison with the long-term prediction of the $foF2$ hourly median values, calculated both at Roquetes and at San Vito using SIRM (Zolesi et al., 1996), and here assumed as quiet-day values. Fig. 2 shows how both at San Vito and at Roquetes the onset of the three considered geomagnetic storms is followed by a positive ionospheric phase (marked in red in Fig. 2)¹ and then, the subsequent day, by a negative phase (marked in blue in Fig. 2) in which $foF2$ is depressed below its median value, as it usually happens at midlatitudes in both hemispheres (e.g. Rishbeth et al. (1987), Prölss (1995), Buonsanto (1999), Villante et al. (2006), Ngwira et al., 2012a,b).

¹ For interpretation of color in Figs. 2–7, the reader is referred to the web version of this article.

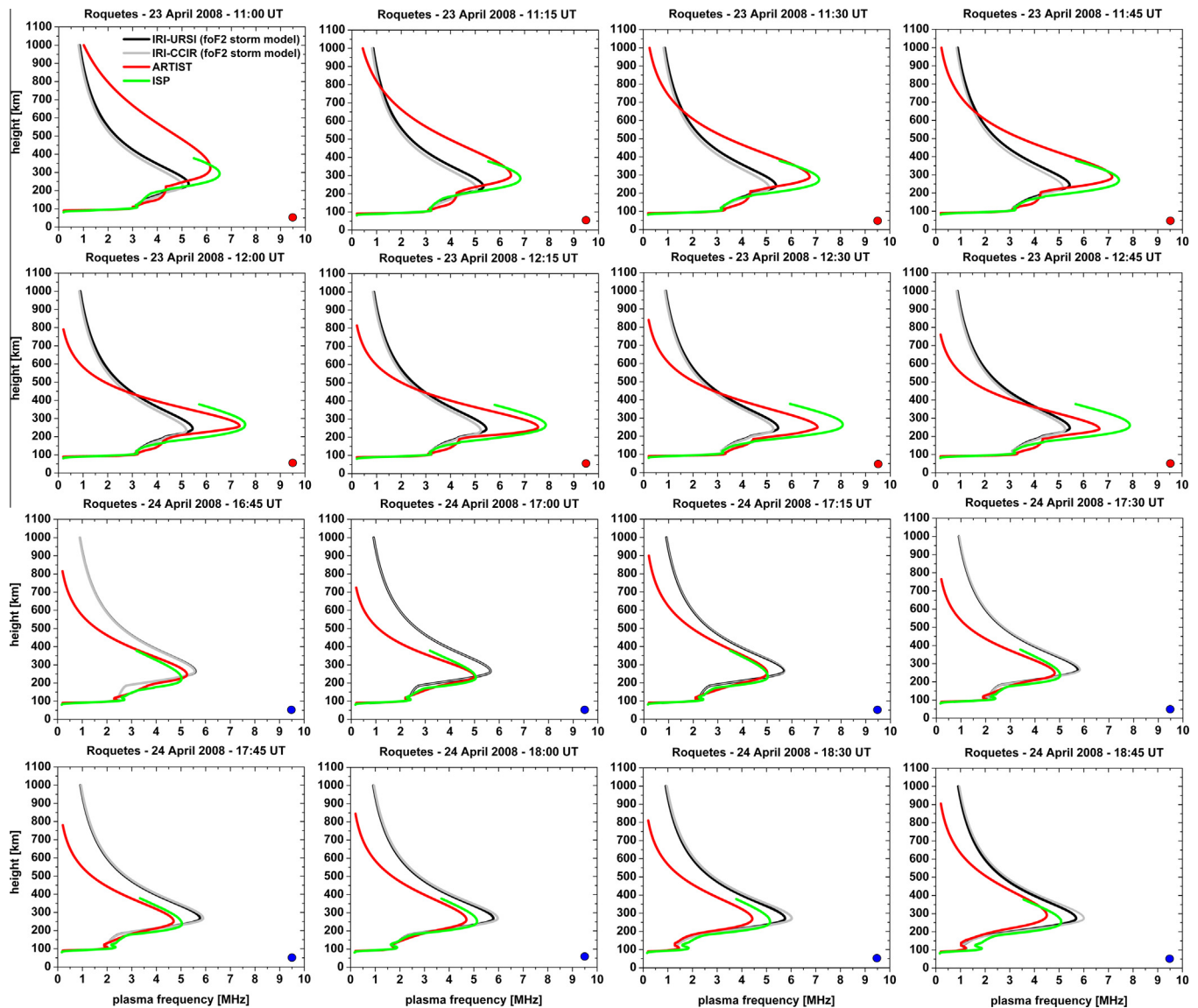


Fig. 4. Same as Fig. 3 for profiles obtained at Roquetes on 23 and 24 April 2008.

The results of the test are shown in Figs. 3–7 where the electron density profiles obtained by the IRI-URSI and the IRI-CCIR procedures, by the ISP procedure, and by the ARTIST system are compared. The IRI-URSI and IRI-CCIR profiles were calculated to a maximum height of 1000 km, using IRI-2007 with the $foF2$ storm model option checked “on” and all the other parameterizations selected as default, while the maximum height of the ISP profiles is equal to 400 km because Autoscala models the topside as a parabolic layer ending right at that height. The ISP matrix from which the corresponding profile at the test site is extracted was calculated by setting $\sigma = 3.0$. This choice of σ following the preliminary testing phase of the model made by Pezzopane et al. (2011). In Figs. 3–7, close to the lower right corner, a red circle identifies profiles belonging to the positive ionospheric phase, while a blue circle identifies profiles belonging to the negative ionospheric phase. Concerning the geomagnetic storm of April

2010, due to the lack of autoscaling data for Rome and Gibilmanna, only the profiles calculated for Roquetes were shown.

Figs. 8a,b and 9a,b illustrate additional results in terms of the differences ($foF2_{ARTIST} - foF2_{ISP}$), ($foF2_{ARTIST} - foF2_{IRI-URSI}$), ($foF2_{ARTIST} - foF2_{IRI-CCIR}$), ($hmF2_{ARTIST} - hmF2_{ISP}$), ($hmF2_{ARTIST} - hmF2_{IRI-URSI}$), and ($hmF2_{ARTIST} - hmF2_{IRI-CCIR}$) of $foF2$ and $hmF2$ (the real height of the maximum electron density of the F2 layer) values obtained at San Vito, and at Roquetes, by the IRI-URSI and the IRI-CCIR procedures, by the ISP procedure, and by the ARTIST system.

4. Discussion and summary

Figs. 3–7 show that the specification of the ionosphere made by the ISP model is far better than the climatological specification made by only either the IRI-URSI or the

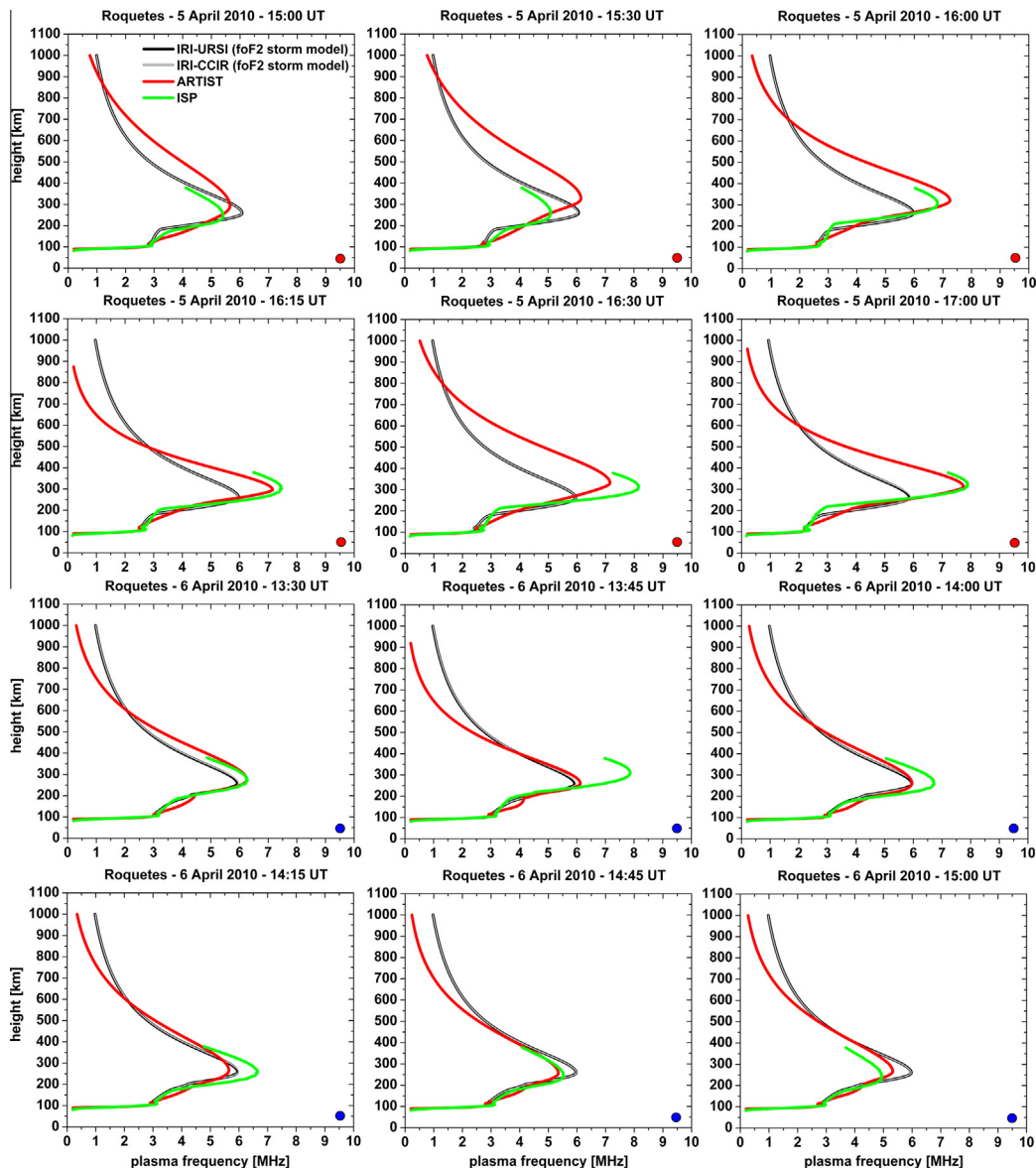


Fig. 5. Same as Fig. 3 for profiles obtained at Roquetes on 5 and 6 April 2010.

IRI-CCIR models. For all the three geomagnetic storms considered in this study, the ISP model can follow pretty reliably the positive and negative phases affecting the ionosphere, both at S. Vito and at Roquetes. The IRI-URSI and the IRI-CCIR models can represent properly only the negative ionospheric phase characterizing the 6 April 2010. On the contrary, Pezzopane et al. (2011) showed that for geomagnetically quiet days, mostly for quasi-stationary ionospheric conditions, the electron density profiles extracted from the IRI-URSI and from the ISP matrixes were pretty similar, and both of them were in good agreement with the electron density profile measured by ARTIST.

This suggests that at the moment for the IRI model the inclusion of the *foF2* storm model is not sufficient to well represent the real conditions of a disturbed ionosphere.

On the other hand, Figs. 3–7 show that the assimilation by IRI of data measured at some reference ionospheric stations is very important to give as output a reliable image of the ionosphere.

Moreover, comparing Figs. 4, 5 and 7 with Figs. 8 and 11 of Pezzopane et al. (2011) it is evident that the inclusion in the ISP procedure of the additional reference ionospheric station of El Arenosillo, which is pretty close to Roquetes, improved noticeably the matching between the profile extracted from the ISP matrix and the profile measured by ARTIST at Roquetes.

However, focusing our attention on some plots, we can see that there are some cases for which the ISP profiles strongly underestimates (see the 5 April 2010 at 15:30 UT of Fig. 5) or strongly overestimates (see the 5 April 2010 at 16:30 UT and the 6 April 2010 at 13:45 UT of Fig. 5)

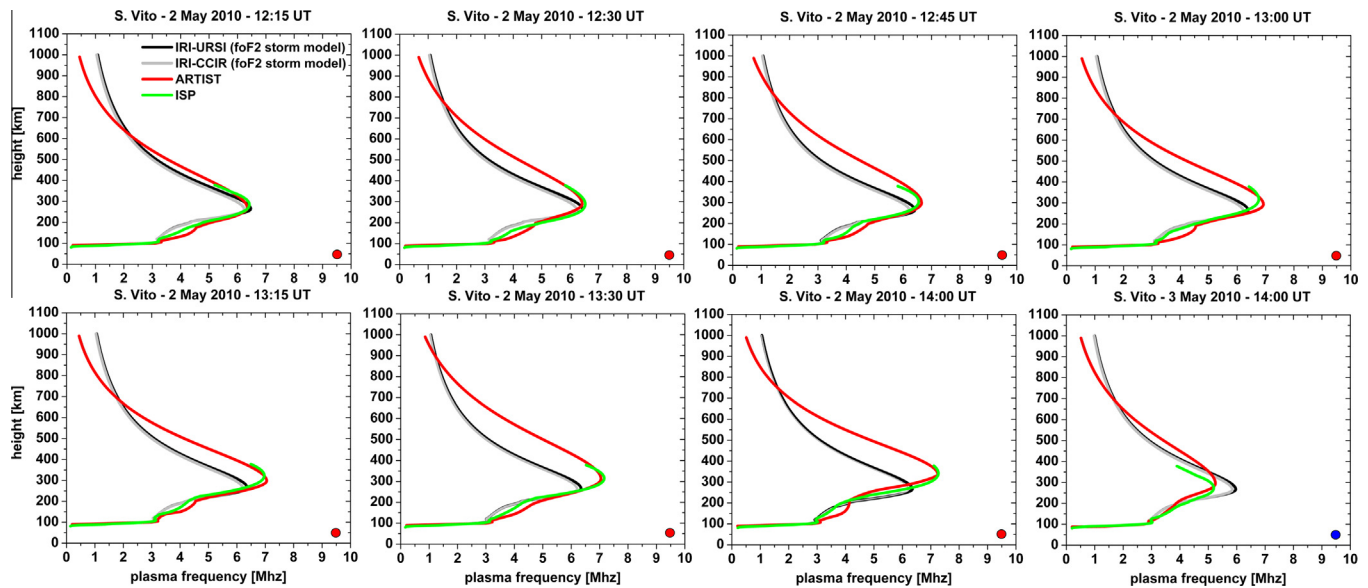


Fig. 6. Same as Fig. 3 for profiles obtained at S. Vito on 2 and 3 May 2010.

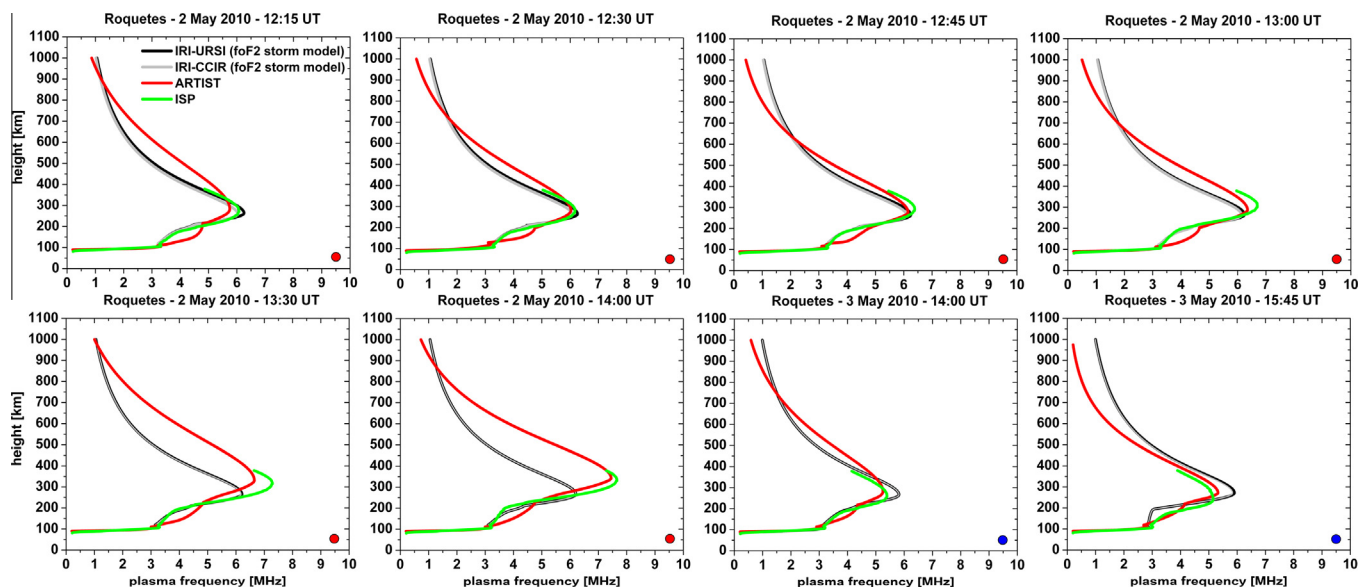


Fig. 7. Same as Fig. 3 for profiles obtained at Roquetes on 2 and 3 May 2010.

the profile measured by ARTIST. In reality, some ISP overestimations are artificial and rather due to an underestimation made by the autoscaling performed by ARTIST that tends to cut off the ionogram trace when this is weak, as it is the case of the ionogram recorded at Roquetes the 5 April 2010 at 16:30 UT (Fig. 10). Looking at Fig. 10, one can see that the trace is weak and does not show any asymptotical trend; the $foF2$ is then truncated at 7.15 MHz, while a more correct value should have been about 7.4/7.5 MHz. With a more correct scaling performed by ARTIST, the overestimation shown by ISP would have been surely smoothed.

With regard to the other overestimations and underestimations that are computed more generally by the ISP

model, these are mainly caused by the large control that the $foF2$ values assimilated by ISP have in the calculation of R_{eff} (Houminer et al., 1993). In fact, if for example the autoscaled $foF2$ values are lower than the long-term $foF2$ values given by SIRM (Zolesi et al., 1996), then the calculated R_{eff} will be lower than the smoothed sunspot number R_{12} that is used by SIRM to calculate the $foF2$ long-term prediction. As a consequence, the $foF2$ and $M(3000)F2$ values of the grid, calculated by the SIRMUP procedure (Zolesi et al., 2004) using this value of R_{eff} , will be overall lower than those given by SIRM, and not only in correspondence of the points of the grid from which the autoscaled $foF2$ values were assimilated. It means that in this case, if in some regions of the grid the real $foF2$ values tend

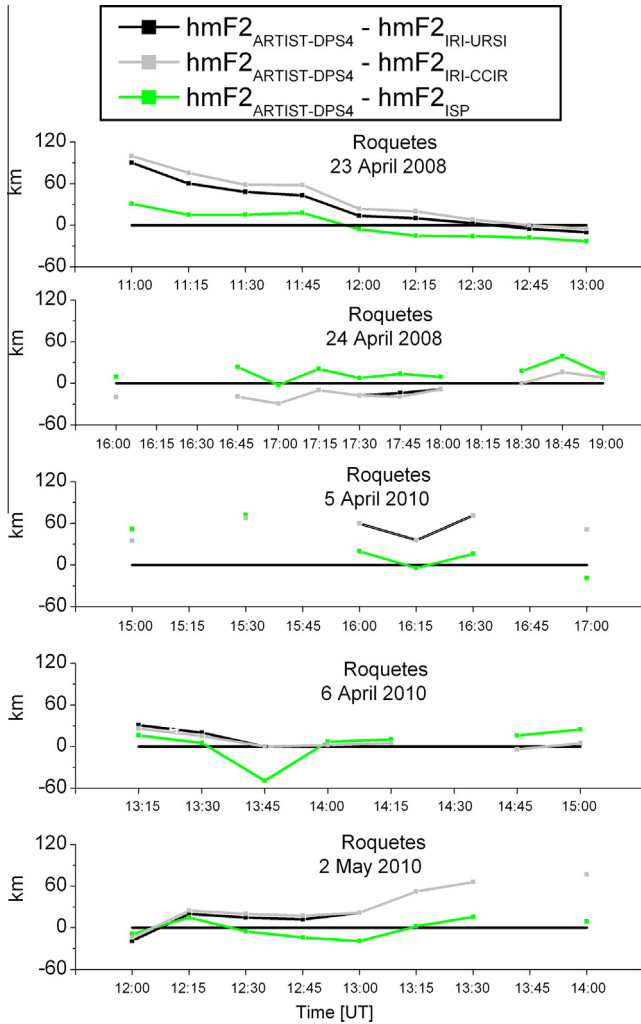


Fig. 8a. Comparison between the differences ($hmF2_{ARTIST} - hmF2_{ISP}$), in green, ($hmF2_{ARTIST} - hmF2_{IRI-CCIR}$), in gray, and ($hmF2_{ARTIST} - hmF2_{IRI-URSI}$), in black, of the $hmF2$ values obtained at Roquetes by IRI-URSI, IRI-CCIR, ISP, and ARTIST for some days of the positive and negative ionospheric phases under investigation.

to be close to the long-term values, the ISP model for those regions will underestimate the real conditions of the ionosphere. This is just what happens at Roquetes on 5 April 2010 at 15:30 UT (see Fig. 5) where the underestimation made by the ISP model is caused by a low value of R_{eff} calculated in virtue of the low $foF2$ values autoscaled at Rome and Gibilmanna.

Vice versa, if for example the autoscaled $foF2$ values are higher than the long-term $foF2$ values given by SIRM, the calculated R_{eff} is higher than the smoothed sunspot number R_{12} that is used by SIRM to calculate the $foF2$ long-term prediction. As a consequence, the $foF2$ and $M(3000)F2$ values of the grid calculated by the SIRMUP procedure using this value of R_{eff} , will be overall higher than those given by SIRM, and not only in correspondence of the points of the grid from which the autoscaled $foF2$ values were assimilated. It means that in this case, if in some regions of the grid the real $foF2$ values tend to be close to the long-term

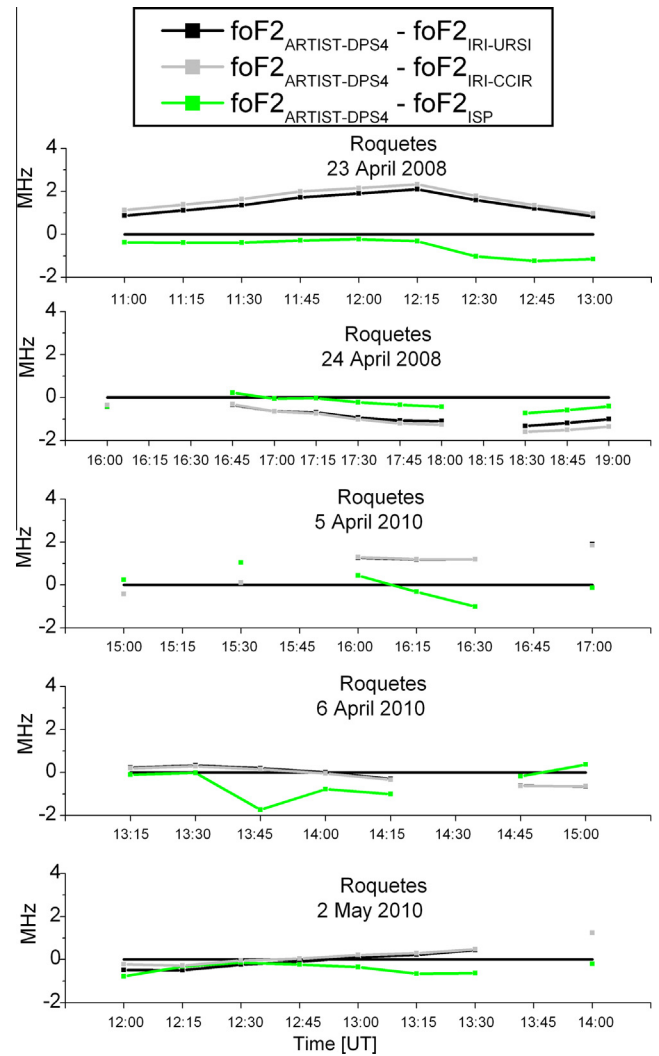


Fig. 8b. Same as Fig. 8a for $foF2$.

values, then for those regions the ISP model will overestimate the real conditions of the ionosphere. This is just what happens at Roquetes on 6 April 2010 at 13:45 UT (see Fig. 5), where the overestimation made by the ISP model is caused by a high value of R_{eff} calculated in virtue of the high $foF2$ value recorded at El Arenosillo.

This kind of problem is of course more likely to happen for disturbed conditions, when the probability to have a very variable ionosphere both in time and in space is greater. The inclusion of additional reference ionospheric stations covering more and more the region mapped by the model could surely smooth out this misrepresentation. For example, in a possible operative utilization of the ISP model, Roquetes and San Vito instead of testing sites would be considered as reference stations, and the overestimations/underestimations just discussed would be surely smoothed out.

Also Figs. 8a,b and 9a,b confirm that the ISP model, even for disturbed conditions, is more representative of the real ionospheric conditions than the standard IRI-

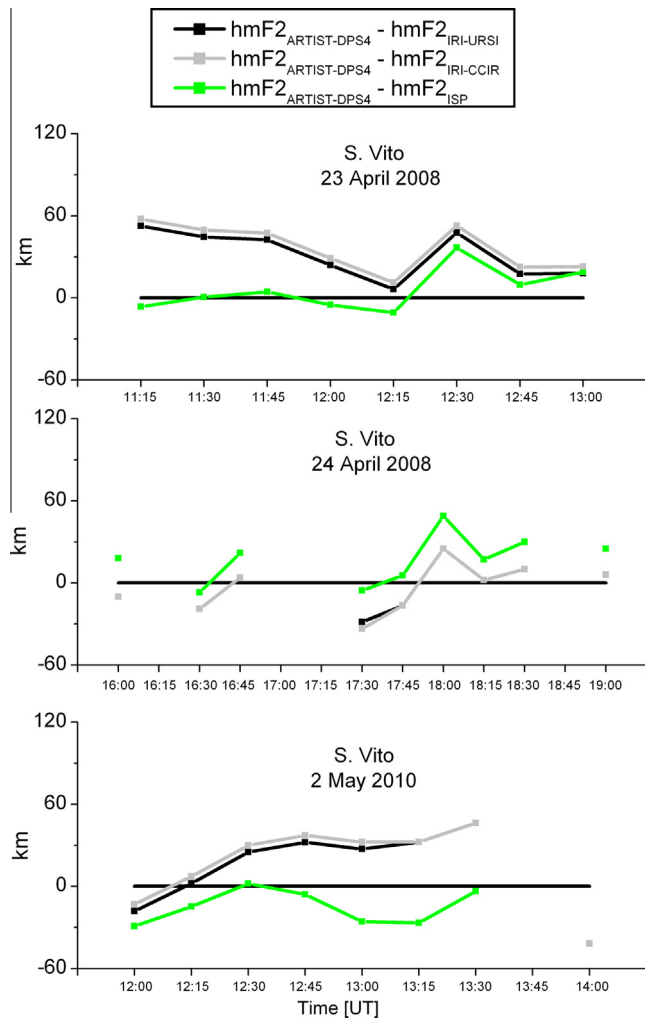


Fig. 9a. Same as Fig. 8a for San Vito.

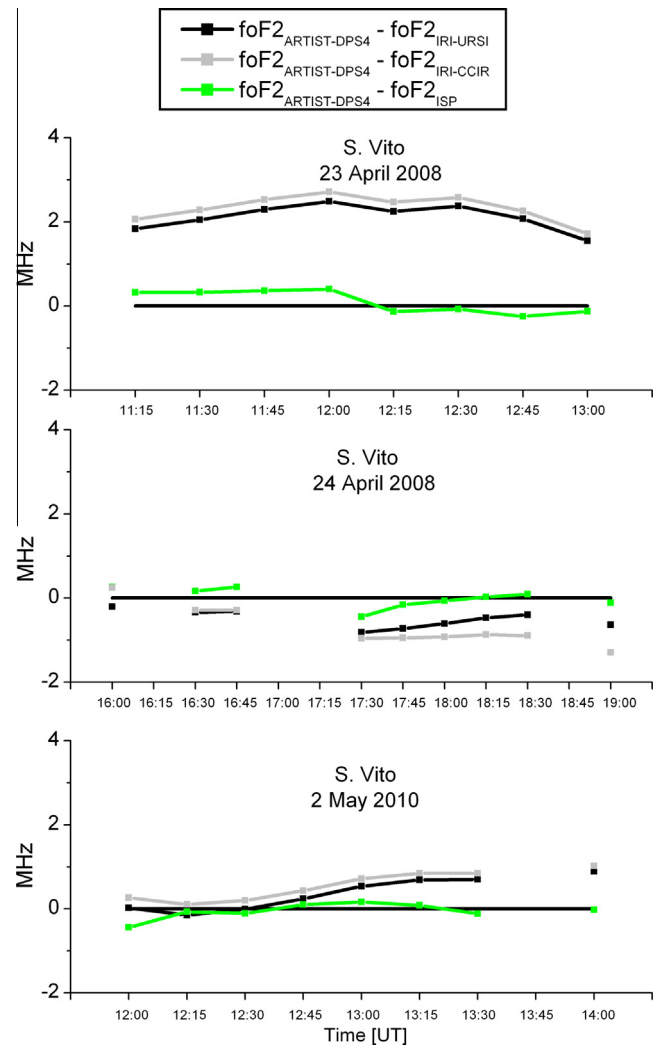


Fig. 9b. Same as Fig. 8b for San Vito.

URSI and IRI-CCIR models. However, concerning these figures, one can note that the $foF2$ values given as output by the model are slightly more reliable than the $hmF2$ values. This is probably due to the fact that the autoscaled $foF2$ values coming from the reference stations are assimilated twice by the ISP model, the first time to calculate a value of R_{eff} , and the second time when the whole vertical electron density profile is assimilated according to Eq. (1). On the contrary, the measured $hmF2$ values are assimilated only when the whole vertical electron density profile is assimilated. Moreover, we have also to take into account that, while $foF2$ is an ionospheric characteristic that is directly measured from an ionogram, on the contrary $hmF2$ is an ionospheric characteristic coming out from the inversion of the ionogram trace, and in general it is affected by a lower accuracy (McNamara, 2008).

Nevertheless, the results shown in this paper demonstrate that the model proposed by Pezzopane et al. (2011) performs rather well also under geomagnetically disturbed conditions, and then it can be considered as a valid tool for obtaining a regional real-time 3-D electron density mapping of the ionosphere. With regard to this regional

feature, it would be interesting to test the ISP model in other regions like for instance South Africa, where the presence of four digisondes installed at Grahamstown (33.3S, 26.5E), Madimbo (22.4S, 30.9E), Louisvale (28.5S, 21.2E), and Hermanus (34.4S, 19.2E), could be exploited to develop a nowcasting regional model based on the assimilation of the $foF2$ and $M(3000)F2$ values autoscaled by ARTIST at these sites. In the framework of the ISP model, this South African regional model could then replace the role played by the SIRMUP model for the Mediterranean area considered in this study, of course considering also the four aforementioned sites as the new reference stations. Also the modeling efforts that have recently been done in South Africa (e.g. Habarulema et al. (2010, 2011) and Sibanda and McKinnell (2011)) could play a significant role for obtaining a reliable 3-D modeling of the South African region.

The goodness of the 3-D electron density representation of the ionosphere computed by ISP will be soon also tested by making use of IONORT (IONospheric Ray Tracing), an applicative software tool for calculating a 3-D ray trac-

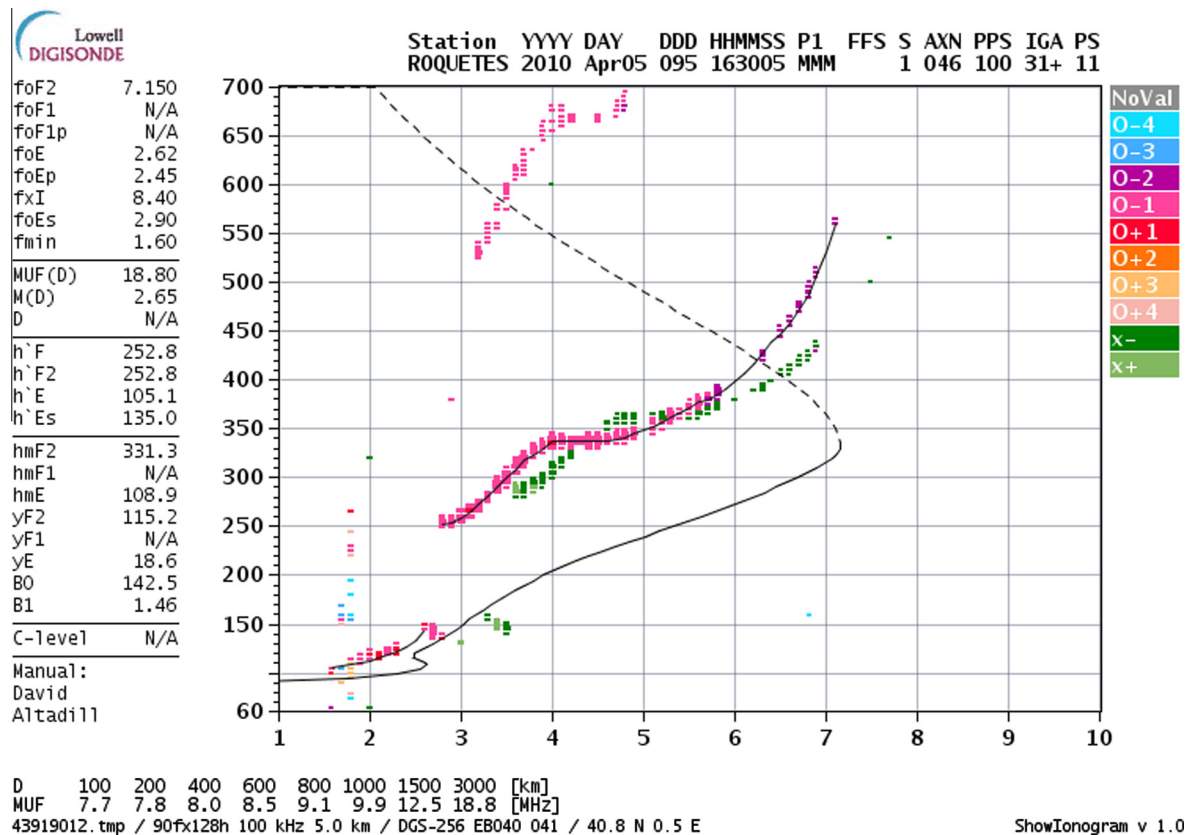


Fig. 10. Ionogram recorded at Roquetes the 5 April 2010 at 16:30 UT. Due to the weakness of the F2 trace, the $foF2$ is truncated at 7.15 MHz, while a more correct value of about 7.4/7.5 MHz should have been output.

ing of high frequency waves in the ionospheric medium (Azzarone et al., 2012). In fact, IONORT gives the user the possibility of choosing among different ionospheric electron density models, having validity in the area of interest. Hence, considering a radio link inside the ISP validity area, for which oblique soundings are routinely carried out, IONORT gives the chance to generate synthesized oblique ionograms over the same radio link. The comparison between synthesized and measured oblique ionograms, both in terms of the ionogram shape and in terms of the maximum usable frequency characterizing the radio path, offers a great opportunity to understand how well the ISP model can represent the real conditions of the ionosphere. This further study will be however presented and discussed in a forthcoming paper.

References

- Angling, M.J., Khattatov, B. Comparative study of two assimilative models of the ionosphere. *Radio Sci.* 41, RS5S20, <http://dx.doi.org/10.1029/2005RS003372>, 2006.
- Azzarone, A., Bianchi, C., Pezzopane, M., Pietrella, M., Scotto, C., Settini, A. IONORT: a windows software tool to calculate the HF ray tracing in the ionosphere. *Comp. Geosci.* 42, 57–63, <http://dx.doi.org/10.1016/j.cageo.2012.02.008>, 2012.
- Bibl, K., Reinisch, B.W. The universal digital ionosonde. *Radio Sci.* 13, 519–530, <http://dx.doi.org/10.1029/RS013i003p00519>, 1978.
- Bilitza, D., Reinisch, B.W. International reference ionosphere 2007: improvements and new parameters. *Adv. Space Res.* 42 (4), 599–609, <http://dx.doi.org/10.1016/j.asr.2007.07.048>, 2008.
- Bradley, P.A. PRIME (Prediction and Retrospective Ionospheric Modelling Over Europe), COST action 238 final report, Commission Of the European Communities, Council for the Central Laboratory of the Research Councils, Rutherford Appleton Laboratory, Didcot, UK, 1999.
- Buonsanto, M.J. Ionospheric storms-a review. *Space Sci. Rev.* 88, 563–601, 1999.
- Decker, D.T., McNamara, L.F. Validation of ionospheric weather predicted by global assimilation of ionospheric measurements (GAIM) models. *Radio Sci.* 42, RS4017, <http://dx.doi.org/10.1029/2007RS003632>, 2007.
- Galkin, I.A., Reinisch, B.W. The new ARTIST 5 for all Digisondes, in: *Ionosonde Network Advisory Group Bulletin*, in: IPS Radio and Space Serv., Surry Hills, N. S. W., Australia, vol. 69, pp. 1–8, 2008. Available also at <<http://www.ips.gov.au/IPSHosted/INAG/web-69/2008/artist5-inag.pdf>>.
- Habarulema, J.B., McKinnell, L.-A., Opperman, D.L. TEC measurements and modeling over Southern Africa during magnetic storms; a comparative study. *J. Atmos. Solar-Terr. Phys.* 72, 509–520, <http://dx.doi.org/10.1016/j.jastp.2010.01.012>, 2010.
- Habarulema, J.B., McKinnell, L.-A., Opperman, D.L. Regional GPS TEC modeling: attempted spatial and temporal extrapolation of TEC using neural networks. *J. Geophys. Res.* 116, A04314, <http://dx.doi.org/10.1029/2010JA016269>, 2011.
- Hanbaba, R. Improved quality of service in ionospheric telecommunication systems planning and operation, COST action 251 final report, Space Research Center, Warsaw, 1999.
- Houminer, Z., Bennett, J.A., Dyson, P.L. Real-time ionospheric model updating. *J. Electr. Electron. Eng., Aust.* 13 (2), 99–104, 1993.

- McNamara, L.F., Decker, D.T., Welsh, J.A., Cole, D.G. Validation of the Utah State University global assimilation of ionospheric measurements (GAIM) model predictions of the maximum usable frequency for a 3000 km circuit. *Radio Sci.* 42, RS3015, <http://dx.doi.org/10.1029/2006RS003589>, 2007.
- McNamara, L.F. Accuracy of models of hmF2 used for long-term trend analyses. *Radio Sci.* 43, RS2002, <http://dx.doi.org/10.1029/2007RS003740>, 2008.
- McNamara, L.F., Baker, C.R., Decker, D.T. Accuracy of USU-GAIM specifications of foF2 and M(3000)F2 for a worldwide distribution of ionosonde locations. *Radio Sci.* 43, RS1011, <http://dx.doi.org/10.1029/2007RS003754>, 2008.
- McNamara, L.F., Retterer, J.M., Baker, C.R., Bishop, G.J., Cooke, D.L., Roth, C.J., Welsh, J.A. Longitudinal structure in the CHAMP electron densities and their implications for global ionospheric modeling. *Radio Sci.* 45, RS2001, <http://dx.doi.org/10.1029/2009RS004251>, 2010.
- McNamara, L.F., Bishop, G.J., Welsh, J.A. Assimilation of ionosonde profiles into a global ionospheric model. *Radio Sci.* 46, RS2006, <http://dx.doi.org/10.1029/2010RS004457>, 2011.
- Ngwira, C.M., McKinnell, L.-A., Cilliers, P.J., Yizengaw, E. An investigation of ionospheric disturbances over South Africa during the magnetic storm on 15 May 2005. *Adv. Space Res.* 49, 327–335, <http://dx.doi.org/10.1016/j.asr.2011.09.035>, 2012a.
- Ngwira, C.M., McKinnell, L.-A., Cilliers, P.J., Coster, A.J. Ionospheric observations during the geomagnetic storm events on 24–27 July 2004: long-duration positive storm effects. *J. Geophys. Res.* 117, A00L02, <http://dx.doi.org/10.1029/2011JA016990>, 2012b.
- Pezzopane, M., Pietrella, M., Pignatelli, A., Zolesi, B., Cander, L.R. Assimilation of autoscaled data and regional and local ionospheric models as input sources for real-time 3-D International Reference Ionosphere modeling. *Radio Sci.* 46, RS5009, <http://dx.doi.org/10.1029/2011RS004697>, 2011.
- Pezzopane, M., Scotto, C. The INGV software for the automatic scaling of foF2 and MUF(3000)F2 from ionograms: a performance comparison with ARTIST 4.01 from Rome data. *J. Atmos. Solar-Terr. Phys.* 67 (12), 1063–1073, <http://dx.doi.org/10.1016/j.jastp.2005.02.022>, 2005.
- Pezzopane, M., Scotto, C. The automatic scaling of critical frequency foF2 and MUF(3000)F2: a comparison between Autoscala and ARTIST 4.5 on Rome data. *Radio Sci.* 42, RS4003, <http://dx.doi.org/10.1029/2006RS003581>, 2007.
- Prölss, G.W. Ionospheric F-region storms, in: Volland, H. (Ed.), *Handbook of Atmospheric Electrodynamics*, vol. 2. CRC Press, Boca Raton, pp. 195–248, 1995.
- Radicella, S.M. The NeQuick model genesis, uses and evolution. *Ann. Geophys. Italy* 52 (3/4), 417–422, 2009.
- Reinisch, B.W., Huang, X. Automatic calculation of electron density profiles from digital ionograms: 3. Processing of bottom side ionograms. *Radio Sci.* 18 (3), 477–492, <http://dx.doi.org/10.1029/RS018i003p00477>, 1983.
- Reinisch, B.W., Huang, X., Galkin, I.A., Paznukhov, V., Kozlov, A. Recent advances in real-time analysis of ionograms and ionospheric drift measurements with digisondes. *J. Atmos. Solar-Terr. Phys.* 67 (12), 1054–1062, <http://dx.doi.org/10.1016/j.jastp.2005.01.009>, 2005.
- Rishbeth, H., Fuller-Rowell, T.J., Rodger, A.S. F-Layer storms and thermospheric composition. *Phys. Scripta* 36, 327–336, 1987.
- Scotto, C. Electron density profile calculation technique for Autoscala ionogram analysis. *Adv. Space Res.* 44 (6), 756–766, <http://dx.doi.org/10.1016/j.asr.2009.04.037>, 2009.
- Scotto, C., Pezzopane, M., Zolesi, B. Estimating the vertical electron density profile from an ionogram: on the passage from true to virtual heights via the target function method. *Radio Sci.* 47, RS1007, <http://dx.doi.org/10.1029/2011RS004833>, 2012.
- Shim, J.S., Kuznetsova, M., Rastätter, L., et al. CEDAR electrodynamics thermosphere ionosphere (ETI) challenge for systematic assessment of ionosphere/thermosphere models: NmF2, hmF2, and vertical drift using ground-based observations. *Space Weather*. 9, S12003, <http://dx.doi.org/10.1029/2011SW000727>, 2011.
- Sibanda, P., McKinnell, L.-A. Topside ionospheric vertical electron density profile reconstruction using GPS and ionosonde data: possibilities for South Africa. *Ann. Geophys.* 29, 229–236, <http://dx.doi.org/10.5194/angeo-29-229-2011>, 2011.
- Thompson, D.C., Scherliess, L., Sojka, J.J., Schunk, R.W. The Utah State University Gauss–Markov Kalman filter of the ionosphere: the effect of slant TEC and electron density profile data on model fidelity. *J. Atmos. Solar-Terr. Phys.* 68 (9), 947–958, <http://dx.doi.org/10.1016/j.jastp.2005.10.011>, 2006.
- Tsagouri, I., Zolesi, B., Belehaki, A., Cander, L.R. Evaluation of the performance of the real-time updated simplified ionospheric regional model for the European area. *J. Atmos. Solar-Terr. Phys.* 67 (12), 1137–1146, <http://dx.doi.org/10.1016/j.jastp.2005.01.012>, 2005.
- Villante, U., Vellante, M., Francia, P., et al. ULF fluctuations of the geomagnetic field and ionospheric sounding measurements at low latitudes during the first CAWSES campaign. *Ann. Geophys.* 24, 1455–1468, 2006.
- Zolesi, B., Cander, L.R., de Franceschi, G. On the potential applicability of the simplified ionospheric regional model to different midlatitude areas. *Radio Sci.* 31 (3), 547–552, <http://dx.doi.org/10.1029/95RS03817>, 1996.
- Zolesi, B., Belehaki, A., Tsagouri, I., Cander, L.R. Real-time updating of the simplified ionospheric regional model for operational applications. *Radio Sci.* 39, RS2011, <http://dx.doi.org/10.1029/2003RS002936>, 2004.
- Zuccheretti, E., Tutone, G., Sciacca, U., Bianchi, C., Arokiasamy, B.J. The new AIS-INGV digital ionosonde. *Ann. Geophys. Italy* 46 (4), 647–659, 2003.